Journal of Engineering Science and Technology
Vol. 15, No. 3 (2020) 1542 - 1561

INVESTIGATION ON CLASSIFICATION EFFICIENCY FOR COAL-FIRED POWER PLANT CLASSIFIERS USING A NUMERICAL APPROACH

FIRAS B. ISMAIL[1,*], NIZAR F.O. AL-MUHSEN[2], RAVEEN LINGAM[1]

[1]Power Generation Unit, Institute of Power Engineering (IPE), Universiti Tenaga Nasional (UNITEN), 43000 Kajang, Selangor, Malaysia
[2]Technical Instructors Training Institute, Middle Technical University, Baghdad, Iraq
* Corresponding Author: Firas@uniten.edu.my

Abstract

Incomplete combustion in boilers often leads to a significant presence of unburnt carbon found in the ash and pollutant emissions. A key factor to overcome this problem is to increase the quality of classification via achieving a greater particle separation quality where at least 70% of the coal particles exiting the classifier are smaller than 75 μm. Three dimensional (3-D) computational fluid dynamics modelling was used to investigate the effect of the steepness of the classifier blade angle on the classification efficiency in Coal-Fired power plants. The gas flow inside the coal mill was solved by the realizable k-ε turbulence model (RKE) with a detailed 3-D classifier geometry meanwhile the discrete phase model was used to solve the coal particles flow. The steepest classifier blade angle of 40^{o} achieved the highest quality of classification where 61.70% of the coal particles are less than 75 μm. Meanwhile, the classification efficiency dipped to 93.0%. An increase in quality of classification leads to a decrease in classification efficiency.

Keywords: Classification efficiency, Classifier blade angle, Quality of classification.

1. Introduction

Improving the system's thermal efficiency has been driven by the concerns of sustainability and environmental protection along with the ever increasingly tightened legislations, which are enforced to reduce greenhouse gas emissions produced by the thermal power plants [1]. Coal classification is the final stage of processing before the combustion of the pulverized ground coal. The ground coal has a wide range of particle sizes ranging from about 75-90 μm according to the mill types. The classifier designed to maintain a limited class of particle sizes and to provide a well-distributed air-coal flow for delivery to the burners [2]. The classification efficiency can be defined as the ratio of the mass of the ground coal entering the coal classifier to that exiting the classifier to the coal burners. Coal classification process has been often overlooked and understudied as the focus of researchers have been drawn towards coal comminution. Coal classification is an essential factor to improve the overall efficiency of the thermal power plant and reduce the concentration of the pollutant emissions from boilers such as the unburned ash, NOx, SOx and CO [3, 4]. The coal classification process can be optimized through two factors which are the quality of classification and classification efficiency. There are several studies were conducted highlighting the effect of the mass flowrate of coal and air, classifier geometry, and the opening of the spiral guide vanes on the coal classification efficiency [5, 6].

It is worth to mention that the optimum quality of classification for coals such as lignite is achieved when 70% of coal particles exiting the classifier is smaller than 75 μm [7, 8]. Other than that, the optimum quality of classification is achieved only when 80% of the coal particles exiting the classifier are finer than 75 μm for the high-ranking coal. Reducing the particles size to the desired limit (≤75 μm) means accelerating the oxidation process of the fineness coal particles, which provides more time for the generated heat from combustion to be transferred to boiler pipes producing a better steam quality and a smaller temperature of exhaust gas emissions. This could potentially decrease the NOx emission and unburned fuel in the produced ash [9]. Fundamentally, the NOx formation is strongly linked with the increase of the combustion temperature [10, 11]. Meanwhile, improving the classification efficiency is essential in reducing the percentage of the coal particles that can be sent back for regrinding [12], which could lessen the operation costs and increase the overall efficiency.

The US Energy Information Administrative (EIA) was drawn a clear figure in the International Energy Outlook 2013 (IEO2013) about the coal consumption that will consistently increase reaching approximately 50% at 2040 starting from 2010 with an annual increase by about 1.3% [13]. According to the IEO2013 report, the major percentage of coal consumption was for power generation purposes. Recently, a new method of collecting samples was used by research groups of Australia (Julius Kruttschnitt Mineral Research Centre) and China (China University of Mining and Technology). Their project was aiming to collect samples for their case studies from both the internal and external of the coal mill. The research group developed mechanistic models based on the collected data for three types of spindle mills comprising a ball-race mill (E-mill), roller-race mill (MPS) and roller-race mill without air classifier (CKP mill) [8, 14]. Özer and Whiten [15] studied the coal breakage in compression tests aiming to obtain the appearance function. This was to give the distribution that results from the breakage of each coal particle type. The outcomes could be used in the

simulation of vertical spindle mills. The authors developed relations that allowed generating a 3-D breakage appearance function for the breakage of both density and size components. The developed relations could be also adopted in coal pulverizer simulation. Özer et al. [16] developed a new model for Vertical spindle mill to interlink the simulation of comminution and classification operations that occur in the mill. The effects of numerous parameters such as the size and ash distribution in coal feed and the consumed power by the mill were incorporated in the multi-component models. The authors concluded that the flow rates and particle size distributions were corresponding to the streams in the mill and its product could be estimated at very good accuracy. Furthermore, the density distributions in these streams could be predicted reasonably. Parham and Easson [17] were investigated the airflow pattern and velocity inside a small-scale coal mill classifier by using three-dimensional Laser Doppler Anemometry. The acquired data were used to enhance the predictions of classifier particle separation and validations of the CFD models.

Coal classifier has been in development due to its potential in improving the overall thermal efficiency of the power plant and the pollutant emissions reduction [2]. It is scientifically essential and more reliable conducting an experimental investigation on such an important topic. Nevertheless, it is costly, and complex to access the real-time operating situation inside the coal classifier. On the other hand, conducting numerical modelling using CFD code with a three-dimensional designed geometry has been proven as a valid tool to explain the mechanism behind the complicated flows inside the coal classifier, which can be only acquired through expensive real-time experiments [18]. Ataş et al. [19] used a three-dimensional CFD modelling to numerically analyse the flow inside the geometry of a vertical spindle mill static classifier at different vane angles. Four designs were numerically analysed, and the best design was chosen and experimentally validated. The numerical results showed that a greater separation efficiency and an increment in the coal mass flow rate to the burner was achieved by using plates to control and direct the flow inside the classifier. Besides, a similar tangential velocity distribution identified in a Cyclone was found in the lower half of the classifier. The findings of [17] showed that the flow regimes, within the classifier, were similar for the Vertical Spindle Model and Cyclone in the lower section of the classifier below a normalized axial, meanwhile above the normalized axial position the regime differed for both models.

The effect of the settings of the classifier vane angle on the coal classification efficiency was numerically investigated by several researchers [2, 20-22]. The effect of inlet air velocity, flow vortex and turbulence on the efficiency of a scaled-down model of a static-air classifier was investigated by using a two-dimensional CFD model [2]. The mixture of gas-coal particle flow inside the crossflow air classifier was simulated based on Euler-Lagrangian approach. Author results showed that the surrounding vane angles could play an important role in enhancing coal classifier efficiency. Shah et al. [20] evaluated the optimum vane angle that provides uniform flow rates and desired coal finesses whereas maximizing the classification efficiency at the outlet pipes. Results showed that at a vane angle opening of 65% was optimal to attain a 60% classification efficiency while the particle size was maintained smaller than 75 μm. Afolabi et al. [22] used a scaled laboratory classifier model to measure the swirl velocity components of the airflow inside the classifier. Three turbulence models, isotropic k-epsilon turbulence

models (RNG k-ε and Realizable k-ε) and anisotropic Reynolds stress model (RSM) were used to numerically evaluate the experimental results. According to the results, the behaviour of the tangential velocity inside highly depends on the inner geometry of the coal classifier. The study concluded that the RNG and RKE models were less accurate than the Reynolds Stress Model (RSM) in the predicting of the gas flow inside the classifier.

By reviewing the extensive researches on multi-dimensional CFD modelling of coal classifier, rare work has been reported on investigating the effect of the classifier blade angle on the classification efficiency with a detailed classifier geometry. This paper represents a numerical investigation to study the effect of the steepness of the classifier blade angle on both classification and particle separation efficiency using turbulent flow models. The classifier model was validated based on quantitative analysis by computing the percentage of the particles' sizes.

2. Geometry Generation

2.1. Significance of static air classifier

Fundamentally, the air classifier inside the coal mill filters the fine coal particles through the loss of momentum caused by the collisions between coal particles and the blades of the classifier [23]. This procedure represents the filtering process of the ground coal whereby the coal classifier allows the finer coal particles to pass through to the boiler to be burned while the heavier coal particles are sent back for regrinding. Accordingly, the classifier blades' design can play an important role in improving the combustion efficiency inside the boiler. Figure 1 shows the selected classifier blade angles for the model of this study which are 70, 60, 50 and 40 degrees. The effect of the classifier blade angles shown in Fig. 1 on the coal classification efficiency is investigated due to its potential to capitalize on the interaction between coal particles and the classifier. A steeper angle of inclination of the blades could increase the potential for collisions between the classifier blades and coal particles leading to a greater quality of classification.

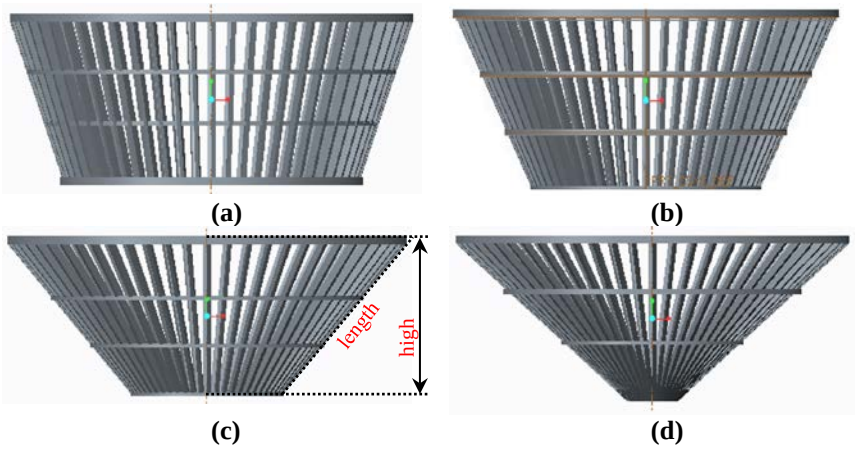

Fig. 1. 3-D model of classifier (Front view) at the tested blade angles of 70º (a), 60º (b), 50º (c) and 40º (d).

2.2. Description of geometry

A multi-dimensional sketch of the used coal pulveriser with an annotated dimension are presented in Fig. 2. The selected coal pulveriser is a rotating bowl and hub coal mill with a power generation capacity of 700 MW(e) using Pipit (061) type coal as fuel. As shown in Fig. 2, the developed geometry consists of three main parts. The first is the classifier body which represents the internal volume of the coal pulveriser. The internal volume is considered to be symmetrical. The second part is the static air classifier that has an original classifier blade angle of 60º. In this study, the blade angle is changed then from 70º to 40º as shown in Fig. 1. The third part of the geometry is the coal outlet chutes where the crushed coal particles exit. Figure 2 also depicts the injection points for the coal and air flowrate.

The working principle of the selected utility is that the coal is supplied through the coal supply chute. The coal is then crushed by stationary crushing blades, a rotating bowl, and hub which continuously applies pressure on the coal particles. A mixture of flue gas from the boiler and fresh air is flowed through the primary air inlet, this mixture of air which has a high velocity carries crushed coal particles into the classifier. The classifier then filters coal particles that are carried by the high velocity stream of air. Larger particles that are not able to pass through will be sent back for regrinding. The fine coal particles then pass through the eight coal outlets into the boiler.

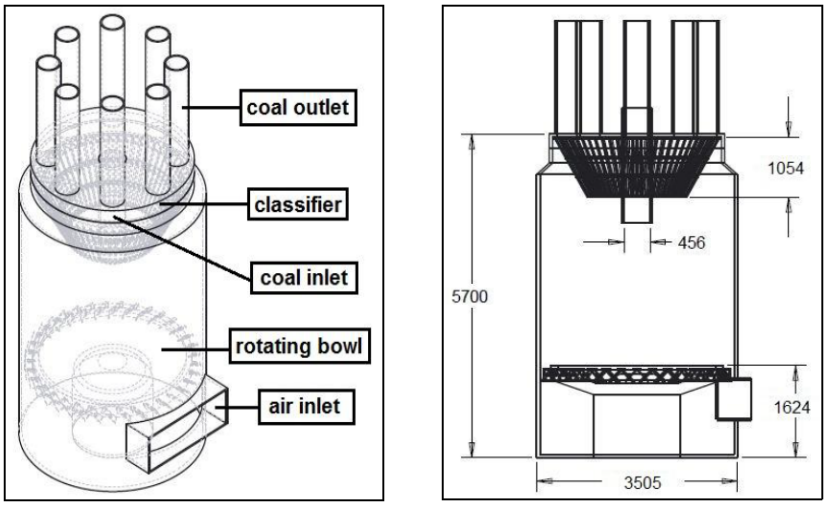

Fig. 2. Schematic diagram for the modelled coal pulverizer with an annotated dimension in millimeter (mm).

2.3. Development of model with varying classifier blade angle

Increasing the mass flow rate of the ground coal particles is a common way to enhance the classification efficiency. This could be achieved by increasing the opening percentage of the classifier blade angle. However, this approach may negatively affect the classification quality via increasing the average coal size particles exiting the classifier. The main hypothesis of this work is to increase the steepness of the classifier blade angle aiming to increase the quality of classification.

Besides, the occurred decrement in the classification efficiency is investigated by developing classifier models with different classifier blades' angles which are 70, 60, 50, and 40 degrees. These four different blade angles are considered for this numerical study due to the model geometry limitations. Because of the classifier height is constrained while the blade angle can be changed, the length of the blade can be calculated accordingly based on Eq. (1).

$$\sin\theta = \frac{hight}{length} \tag{1}$$

The classifier blade length has been calculated according to each blade angle as shown in Table 1. When the classifier blade angle decreases with respect to the x-axis of the used model, the length of the classifier blade increases accordingly. When the classifier blade angle decreases by 30^{o} from 70° to 40°, the blade length increases by about 37 mm. The results of the associated effect of blade angles and the consequent increment in the blade length on the classification quality and efficiency are comprehensively discussed and analysed.

Table 1. Geometry dimension of the developed model including classifier height, proposed blade angles and the blade lengths.

Classifier Blade Angle (^{o})	Height (mm)	Length of Blade (mm)
70	75	79.78
60	75	86.61
50	75	97.91
40	75	116.82

2.4. Assumptions in geometry creation

During the development process of this model, assumptions have been made in order to simplify the creation of the model geometry and simulate the mixture flow of the hot air and coal particles inside the coal mill. These assumptions are listed and explained as follow.

2.4.1. Neglecting the effect of the rotating hub and crusher

The main focus of this study is to numerically investigate the interaction between the crushed coal particles and classifier blades. Therefore, the geometry effect of the crushing rotary blades (rotating bowl and hub) of the used coal mill have been neglected in the development and drafting of the used model. Since the effect of the geometry of the crushing blades on the flow field of hot air and coal particles mixture is very small, it can be neglected. Hence, the processing time of the numerical simulation caused by the complex design of the crushing blades could be significantly reduced.

2.4.2. Re-positioning the inlet for coal supply

Unlike the original model, in this model simulation, the coal particles are injected to the classifier from the bottom surface of the designed geometry. If the coal particles are injected from the top, a backflow of the injected coal particles into the inlet chute might occur [24]. In order to overcome this issue, the injection position of the coal particles is changed from the top to the bottom surface of the model. Avoiding the backflow of the coal particles could cause deviations during data

validation when the actual plant data are used. It worth to be mentioned that, re-positioning the inlet coal supply would only have a negligible effect on the actual internal flow field of air and coal particles.

2.4.3. Uniform distribution of coal particles

The coals particles were injected with an equal distribution from the bottom of the model with an upward trajectory and a specified total mass flow rate. This is for mimicking the behaviour of coal particles after undergoing grinding process by the bowl and hub. Although this is not how the coal particles behave inside the coal pulveriser in the actual cases, this assumption is still reasonable for the case of this study. This is because the mass flow rate of coal particles with respect to the particle diameter distribution at the outlet is desired. Therefore, the coal particles have been assumed to be completely ground [25]. Besides, it was assumed that the pulverized coal particle would follow the air stream inside the coal mill as long as the lift forces provided by the hot air supplied from the boiler exceeds the gravitational force of each carried coal particle in the stream [9]. The flow can be also considered as a dilute mixture because the amount of inert particles is less than 10% of the air [26].

3. Data Preparation for Model Validation

In order to validate the developed model accurately, real-time finesses' results of the Jana Manjung Power Plant Station [27] for October 2016 were used as a benchmark. Jana Manjung Power Plant Station has a power capacity of 4.1 GW and it is a coal-fired power facility. It is originally developed with three 700 MW units before it was further expanded by two 1000 MW ultra-supercritical units. For this study, the quality of classification for the selected power plant was 61.51% while the classification efficiency was 99.30%.

3.1. Computational domain

In this study, the flow of the mixture (coal particles and hot air) inside the coal mill and classifier was numerically investigated. The computational grids were modelled using the pre-processor Design Modeller before meshing the computational grids. The numerical simulation was performed through the CFD code ANSYS Fluent version 16.0. In order to obtain a good quality computational results, 4×10^6 grid cells were used for the geometry meshing and simulation. The maximum face size used per grid was 10 mm, while the minimum face size per grid was set at 0.02 mm. The tetrahedral fine grids were chosen due to its tolerance for the unstructured meshing [28], as shown in Fig. 3. Although previous numerical studies suggested larger number of cells that might lead to more accurate results [5, 9, 19], 4×10^6 grid cells were chosen due to the time limitations of the CFD processing. Figure 3 shows the cross-sectional view of the internal part of the meshing grid. The coal classifier is highlighted in the green colour as shown in Fig. 3 between the multi-dimensional geometry of the coal mill and the 3-D view of the meshing grid. This is to highlight that the flow of gas-particle mixture (ground coal and air) is meshed and modelled. This to tackle the coal particles being separated by the coal classifier. To increase the accuracy of the performed CFD simulation of this study, the size was chosen carefully based on the deviation of the results between the experimental and numerical results. The mesh size that yields the smallest deviation results was selected for this study. Besides, different mesh sizes

were tested in order to reduce the computational error and time. The smallest results deviation with less than 1% was achieved when the mesh size was 4×10^6 cells at the two-phase flow of the mesh independent test.

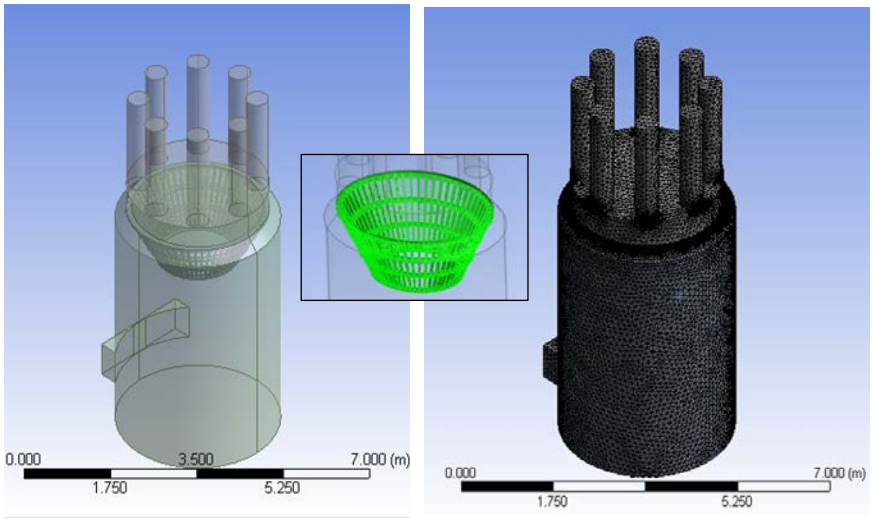

Fig. 3. Multi-dimensional view of the coal mill geometry and a 3-D view of the meshing grid.

3.2. Numerical method

In this work, a numerical model was developed using ANSYS Fluent. In general, inside the coal classifier, the nature of the flow of the air-coal mixture is turbulent due to the design and working mechanism of the classifier. Therefore, an accurate turbulence model should be adopted to simulate the flow inside the coal pulverizer. Accordingly, the Reynolds Averaged Navier-Stokes (RANS) equations were used in the numerical simulation of this study and similar investigations [2, 29]. The Reynolds-averaged (or time-averaged) continuity and momentum equations could be listed as follows:

$$\frac{\partial \rho}{\partial t} + \frac{\partial}{\partial x_i}(\rho u_i) = 0 \tag{2}$$

$$\frac{\partial}{\partial t}(\rho u_i) + \frac{\partial}{\partial x_j}(\rho u_i\, u_j) = -\frac{\partial p}{\partial x_i} + \frac{\partial}{\partial x_j}\left\{\mu\left(\frac{\partial u_i}{\partial x_j} + \frac{\partial u_j}{\partial x_i} - \frac{2}{3}\delta_{ij}\frac{\partial u_i}{\partial x_i}\right)\right\} + \frac{\partial}{\partial x_j}\left(-\overline{\rho u_i' \rho u_j'}\right) \tag{3}$$

The term of the turbulence stress, $\left(-\overline{\rho u_i' \rho u_j'}\right)$, that appeared in Eq. (3), was be modelled in this study to provide a closed set of equations for the turbulence flow inside the coal pulverizer [2].

The realizable k-epsilon (RKE) turbulence model was used to simulate the gas flow inside the coal mill and classifier. The RKE turbulence model was developed based on the standard *k-ε* model. It was formulated based on specific turbulent dissipation rate *ε*, with a new formulation for turbulent viscosity. The *Cμ* variable and turbulence variables (i.e. *k, ε*) are sensitized to the mean flow, and hence the mean rotation is considered. Therefore, it is considered that the RKE model, shown in Eqs. (4) and (5), is capable to simulate the turbulent flow with a strong streamline curvature, vortices, and rotation as well [30]. Consequently, in this study, the RKE

model can be used in solving gas-solid turbulent flow in classifier with high turbulence. The turbulent kinetic energy (k) equation is represented in Eq. (4) and turbulent dissipation rate (ε) in Eq. (5) [29].

$$\frac{\partial}{\partial t}(\rho k) + \frac{\partial}{\partial x_i}(\rho k u_i) = \frac{\partial}{\partial x_j}\left\{\left(\mu + \frac{\mu_t}{\sigma_k}\right)\frac{\partial k}{\partial x_j}\right\} + P_k + P_b - \rho\varepsilon - Y_m + S_k \quad (4)$$

$$\frac{\partial}{\partial t}(\rho\varepsilon) + \frac{\partial}{\partial x_i}(\rho\varepsilon u_i) = \frac{\partial}{\partial x_j}\left\{\left(\mu + \frac{\mu_t}{\sigma_\varepsilon}\right)\frac{\partial \varepsilon}{\partial x_j}\right\} + C_{1\varepsilon}\frac{\varepsilon}{k}(P_K + C_{3\varepsilon}P_b) - \rho C_{2\varepsilon}\frac{\varepsilon^2}{k} + S_\varepsilon \quad (5)$$

where turbulent viscosity, $\mu_t = \rho C_\mu \frac{k^2}{\varepsilon}$, production of k, $P_k = -\overline{\rho u_i' u_j'}\frac{\partial u_j}{\partial x_i}$, effect of buoyancy, $P_b = \beta g_i \frac{\mu_t}{Pr_t}\frac{\partial T}{\partial x_i}$ and $\beta = -\frac{1}{\rho}\left(\frac{\partial \rho}{\partial T}\right)_p$. The buoyancy effect ($g_i$) represents the gravitational vector in the i^{th} direction and Pr is the turbulent Prandtl number. For the standard and realizable k-epsilon turbulent models, the Pr value is 0.85. Standard Wall Functions was used for the near-wall treatment [28]. The mass, energy and momentum conservation equations between the mill walls and flow of air and coal particles were numerically solved under steady state conditions. Meanwhile, the particle flow was solved using the discrete phase model (DPM) and Rosin-Rammler distribution function to simulate coal particles ranging from 25- 300 µm. The DPM was valid because the mixture was diluted [26]. The numerical simulation settings were carried out repeatedly at different coal classifier blade angles. The main used settings and the operating conditions of the used coal mill for the CFD simulation in this study are listed in Table 2, as follows.

Table 2. Numerical investigation settings.

Input	Parameter
Particle Injection	Surface
Particle Type	Coal-Hy (Pipit)
Distribution	Rosin-Rammler
Coal Flow Rate (kg/s)	15.0
Min Diameter (µm)	25.0
Mean Diameter (µm)	75.0
Max Diameter (µm)	300.0
Spread Parameter	3.5
Air Mass Flow Rate (kg/s)	30.0
Gravity (m/s^2)	9.8

Figure 4 shows the simulated model for this study and the corresponding boundary conditions. The coal particles were set in this simulation to be injected from the base of the model to simulate the flow of ground coal being blown upward toward the classifier. The two inputs of the model were set as a mass flow dependant, meanwhile, the output was set as a pressure dependant. The first input was set for the inlet hot air that is blown from the bottom of the model with a flow rate of 30.0 kg/s while the second input was the mass flow rate of the ground coal at 15.0 kg/s. The outlet pressure was set to be at the atmospheric pressure level of 101.325 kPa.

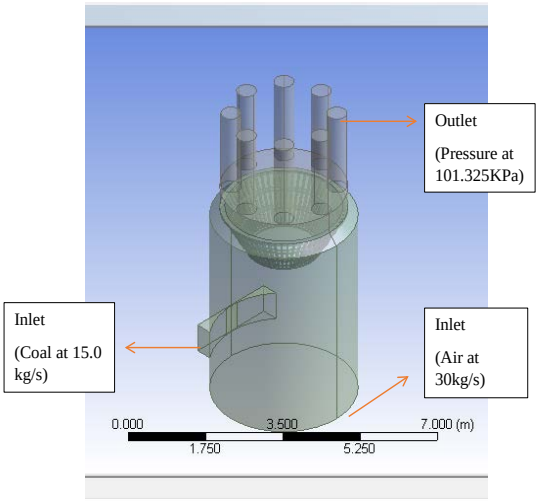

Fig. 4. The simulated model of the coal mill and classifier with the boundary conditions set.

3.3. Mesh independent study

In order to validate the grid size and the CFD simulation settings, a mesh independent study was carried out for the used coal mill model in this study. It is well known that a simulation model with a sufficiently fine mesh is able to capture the flow features with higher accuracy. As shown in Fig. 4, the used model consists of two inlets and one outlet. The mesh independence study was divided into two stages. Firstly, a single-phase airflow simulation was adopted in the first stage. The air was perpendicularly injected with a velocity of 16 m/s to the surface of the inlet boundary. The averaged air velocity at each outlet was then obtained. The used mesh was ranging from 2×10^6 cells (coarse mesh) to a fine mesh made of 10×10^6 cells. It can be noticed from Fig. 4 that the captured velocity values were inconsistent when the number of meshes was between 2×10^6 to 3×10^6 cells. However, the velocity magnitude was consistent when the cell number was beyond 4×10^6. Therefore, the meshes number of 4×10^6 was chosen for further CFD simulation of the proposed model of this study.

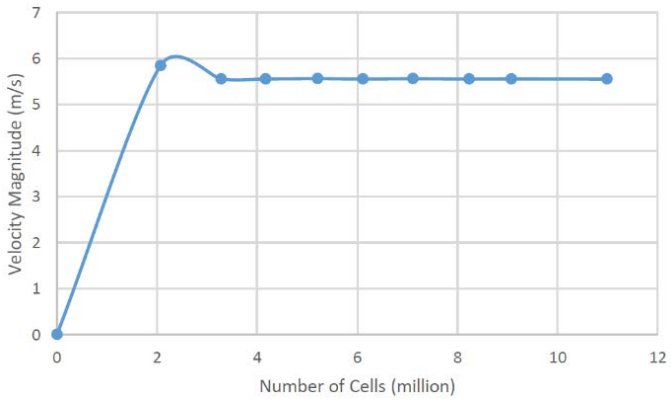

Fig. 5. Air velocity magnitude for single phase mesh independent test.

Secondly, the two-phase flow of air and coal particles that were sizing from 25 – 300 μm was perpendicularly injected to the inlet port of the model with a mass flow rate of 13.52 kg/s. The mean value of the coal fineness was obtained at the coal outlet. Similar to the single-phase flow mesh independent study, the mesh size of the two-phase flow testing was ranging from 2×10^6 - 4×10^6 cells. In order to determine the most suitable mesh size, the results of the simulated coal fineness were compared with the experimental data. The mesh size that yields the smallest deviation between the simulation and experimental results was selected for this study. As shown in Table 3, the model with 2×10^6 cells demonstrated the greatest deviation > 10 % between the simulation and experimental results. On the other hand, the fine mesh with 4×10^6 cells exhibited a minimum deviation with less than < 1 %. Consequently, the simulation model with 4×10^6 cells was considered to be suitable for the subsequent simulations, as the model could provide a reasonable accuracy at a minimal computational effort.

Table 3. Coal fineness results for two-phase flow grid independence test.

Coarse Mesh: 2,000,000 cells			
Particle Diameter (μm)	**Experimental (%)**	**Simulation (%)**	**Deviation (%)**
>75	38.24	46.00	16.87
<75	61.76	54.00	12.56
Fin Mesh: 4,000,000			
Particle Diameter (μm)	**Experimental (%)**	**Simulation (%)**	**Deviation (%)**
>75	38.24	38.50	0.68
<75	61.76	61.50	0.42

4. Results and Discussions

4.1. Numerical model validation

Figure 6 shows the particle diameter distribution at the outlet for a classifier blade angle of 60 degrees. It can be seen that the red arrow in the Histogram of particles distribution represents the particle with size of 75 μm (X = 75μm). The region to the left of the shaded line represents the particle sizes ranging from 25 μm to 75μm, meanwhile, the region to the right of the shaded line represents particles from size 75 μm to 120 μm. The percentage of the particles that have a size of less than 75μm are considered as fine particles while the percentage of particles that have a size of more than 75 μm are considered as coarse particles. The calculated percentage of the particle distribution for the simulated model and the deviations between experimental and simulation results are then listed in Table 4. Table 4 shows the percentage of the coal particles with larger than 75 μm are 40.70% meanwhile the percentage of the particles with smaller than 75 μm is 57.50% for the simulated model. However, these percentages for the developed model are slightly different from the experimental results. For the experimental model, the coal particles percentage are slightly decreased to 37.85% at X > 75 μm but it increases to 61.51% at X < 75 μm. The maximum deviations between simulated and experimental results are 7.53% and 6.51% which are within the acceptable range [31]. This demonstrates the acceptable results of the developed model.

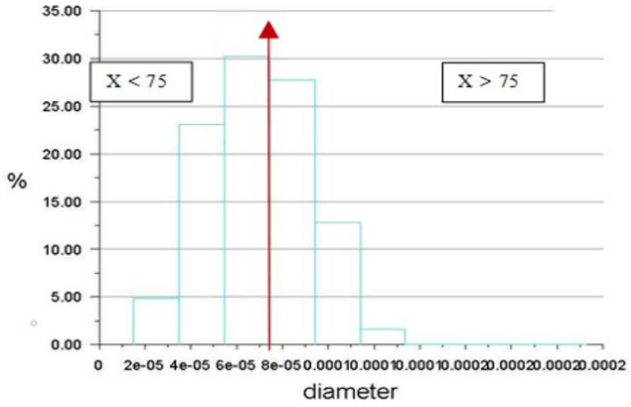

Fig. 6. Histogram of particle distribution at 60º blade angle.

Table 4. Summary of the experimental results and CFD model validation.

Particle Diameter (µm)	Experimental (%)	Simulation (%)	Deviation (%)
***X*>75**	37.85	40.70	7.53
***X*<75**	61.51	57.50	6.51

4.2. Justifications on deviations

As shown in Table 4 and Fig. 6, there is a considerable difference between the experimental and numerical simulation results according to the size of the coal particle diameter. This might be mainly attributed to the three main reasons. Firstly, the coal particles were assumed to be injected with an equal distribution from the bottom of the model with an upward trajectory and total mass flow rate of 15 kg/s. The coal particle diameter distribution was distributed using the Rosin-Rammler equation in the ANSYS Fluent. This was to tackle the behaviour of the coal particles after undergoing grinding process by the bowl and hub.

The assumed aforementioned settings could significantly contribute to the occurred deviations in the obtained results. Secondly, disregarding the effect of the crusher blades and bowl could also affect the attained numerical results. Ignoring the interaction of coal particles with these geometries within the coal mill might strongly contribute to the deviations between the actual and numerical results. This could be due to coal particles losing momentum produced by lift to elastic collisions with the crusher blade and bowl. This might cause the coal particles to lose drag force and spending more time inside the classifier which could be resulting in the difference between the real-time and numerical results, as shown in Fig. 6 and Table 4.

Thirdly, in this study, the flow of the coal particles was solved using the DPM equations but particle to particle interaction was not considered as it would increase the cost of the computational process. Within the classifier, particle to particle interaction could cause the coal particles to lose momentum due to losing the lift energy during collisions with other coal particles. The exclusion of particle to particle interaction during simulation could also play an important role in the results' deviation.

4.3. Effect of classifier blade angle on classification efficiency

The classification efficiency was calculated based on Eq. (6) and by using the DPM model tracking in the ANSYS Fluent. The flow of coal particles at the injected inlet and at the outlet ports was tracked, and the number of the particles at each port was counted as well to calculate the classification efficiency accordingly.

$$Class.Eff. = \frac{Total\ coal\ mass\ at\ outlet}{Total\ coal\ mass\ at\ inlet} = \frac{No.of\ coal\ particles\ escaping}{Total\ No.\ of\ coal\ particles\ injected} \quad (6)$$

The effect of four classifier blade' angles was numerically tested in this work and the attained results shown in Figs. 7 which are discussed and analysed. Figure 7(a)-(d) demonstrates the distribution of the coal particles at the outlet for a classifier blade angles of 70, 60, 50 and 40 degrees respectively according to the size of the coal particles. The measured size of the coal particles using the CFD method is ranging from 25 μm to 120 μm, as shown in Figs. 7(a)-(d). It can be noticed that the finest particles, which have a size less than 75μm, increase with the reduced blade angle from 70° to 40°. However, there is no significant difference between the blade angle of 70° and 60° in terms of the percentage of the calculated fine coal particles. The maximum percentage of the fine particles is achieved when the blade angle is 40° meanwhile the minimum occurs at the blade angle of 70°. This could significantly enhance the quality of classification as shown in Fig. 9, but it reduces the efficiency of the ground coal classification, as shown in Fig. 8.

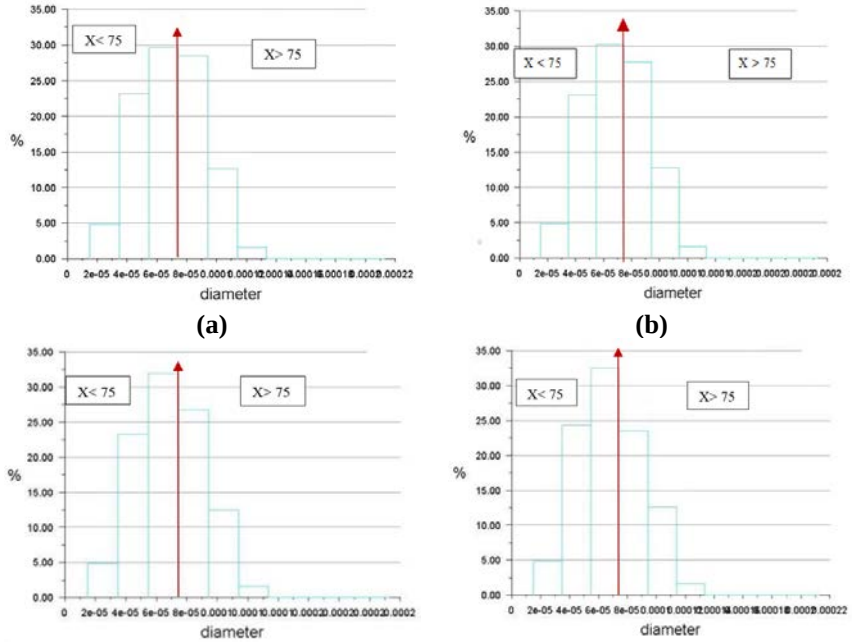

Fig. 7. Histogram of particle distribution at the tested blade angles of 70° (a), 60° (b), 50° (c) and 40° (d).

Figure 8 shows that the classification efficiency verses the classifier blade angle at the tested conditions. It can be noticed that the efficiency decreases when the

classifier blade angle decreases. This could be attributed to the reduced surface area where the coal particles passing through. According to the settings of the simulation of this study, an equal number of coal particles was injected at the inlets of the coal mill which is 123,110 particles for all the used four models of classifier blade angles of 70, 60, 50, and 40 degrees. However, the number of particles escaping tend to be reduced when the blade angle is decreased from 70 to 40 degrees. The model that allowed the greatest number of particles to escape through it is the model with a classifier blade angle of 70° which allowed around (120,717) particles to be passed through. On the other hand, the model with an angle of 40° allows the lowest number of coal (114,615) particles escaping through it. At blade angles of 60, 50 and 40 degrees, the numbers of the escaped coal particles through the classifier decrease by 1.14%, 2.51%, and 5.05% respectively compared with that of 70° classifier angle. Therefore, it can be noticed that the classification efficiency is inversely proportional to the steepness of the classifier blade angle.

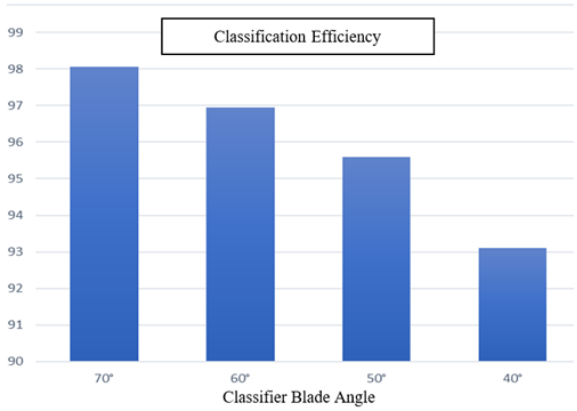

Fig. 8. Classification efficiency for different classifier blade angles.

4.4. Effect of classifier blade on quality of classification

The effect of the classifier blade angle on the quality of classification is analysed by computing the percentage of the coal particles that are finer and coarser than 75µm at the outlets of the coal mill, as shown in Fig. 9. It is well known that the optimum quality of the ground coal classification is achieved when at least 70% of the coal particles at the outlet have a smaller diameter than 75 µm [7, 8]. The quality of classification, which is the percentage of coal particles that are finer than 75µm, increases as the classifier blade angle decreases (increased in steepness). As shown in Fig. 9, the quality of classification increases from 56.7% to 61.7% as the blade angle is reduced from 70 to 40 degrees. This is because as the angle is reduced the steepness of the blade on the classifier also reduces. This causes a decrease in the surface area of the classifying zone. This decrease in the classifier surface area can lessen the number of coal particles, which are coarser than 75µm, that are passing through the classifier to the outlet ports. Moreover, the decrease in surface area of the classifying zone could also increase the interaction between the coal particles and blades of the classifier. This collision between the classifier blade and coal particles could cause the coal particles to lose their momentum. Therefore, it can be deduced that the classifier blades steepness and the quality of classification are directly proportional.

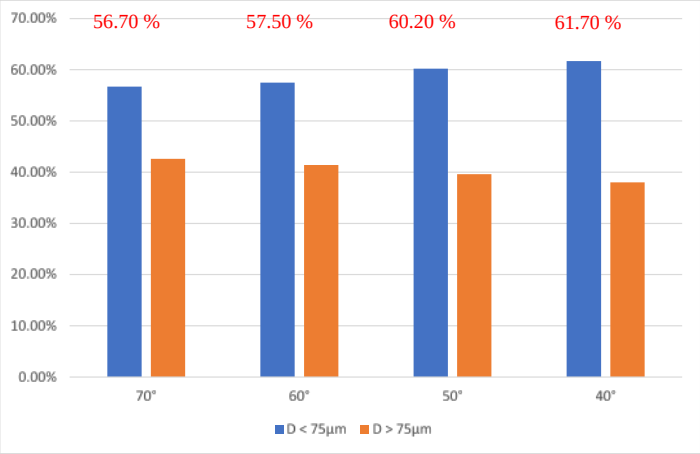

Fig. 9. Histogram for quality of classification.

4.5. Effect of classifier blade angle on the flow of gas-particles

For validation of the simulated model, the simulation was performed first on a classifier that has an original classifier blade angle of 60º and using the numerical analysis parameters defined in Table 2. In this work, all coal particles ranging from (25 µm to 300 µm) were injected from the bottom surface of the mill geometry. The qualitative analysis in Fig. 10 shows the flow path of different sized particles that starting from the bottom surface, passing throughout the classifier and then ending with the exit ports. It can be observed that the percentage of the large coal particles represented by the red track is significantly less than the percentage of the finer coal particles represented by the green and blue tracks.

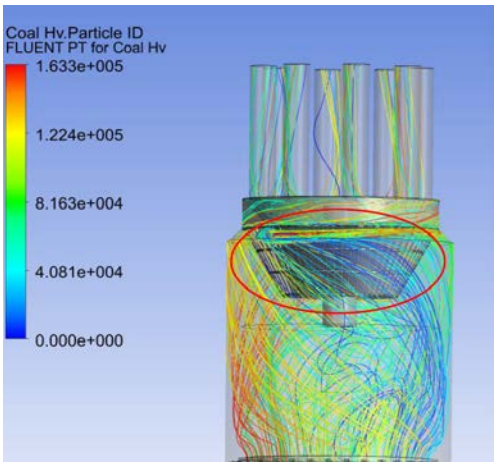

Fig. 10. Flow visualization at classifying zone.

The flow patterns of gas-particle for classifiers' blades angles of 70, 60, 50, and 40 degrees are presented in Figs. 11(a)-(d) respectively. Although, the flow patterns tend to be similar when the blade angles are 70 and 60 degrees, as shown in Figs. 11(a) and (b) respectively, in both the isometric and top view. This could be mainly

attributed to the small difference in the number of the fine coal particles that passed through the classifier, which was calculated as less than 1.5%. On the other side, a substantial difference takes place at the flow pattern of the coal particles inside the classifier that has a blade angle of 40º compared with that of 70º. This is because larger numbers of finest coal particles escape the classifier when the blade angle is reduced to 40º. A greater concentration for the particles' tracks represented by the dark blue colour, which represents the fine coal particles, at the centre of the classifier can be observed when the blade angle is 40º. The classifying quality is the highest in the middle that is represented in the bottom region of the conical classifier. This could be due to the smaller surface area that is available for the finest coal particles to pass through at the lower surface region of the classifier towards the outlet ports, as shown in Fig. 10.

As shown in Fig. 11, when the classifier blade angle decreases, the concentration of blue particle tracks at the centre region increases. Comparing Figs. 11(a), (b) and (c), it can be clearly noticed that the concentration of blue particles tracks at the centre is higher in Fig. 11(c) than that of Figs. 11(a) and (b). Furthermore, in Fig. 11(d), a black area inside the classifier can be observed. This could be explained as there are no particles have passed through this region during the running time of this study simulation. This is highly consistent with the numerical findings when the classifier blade angle decreases, the surface area for particles to pass through also becomes smaller.

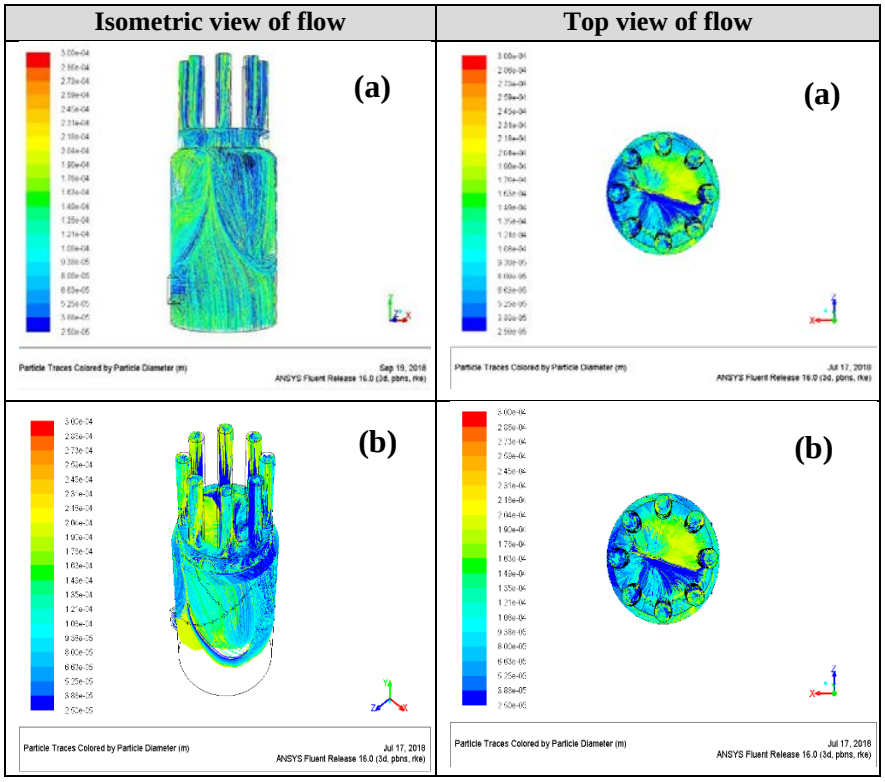

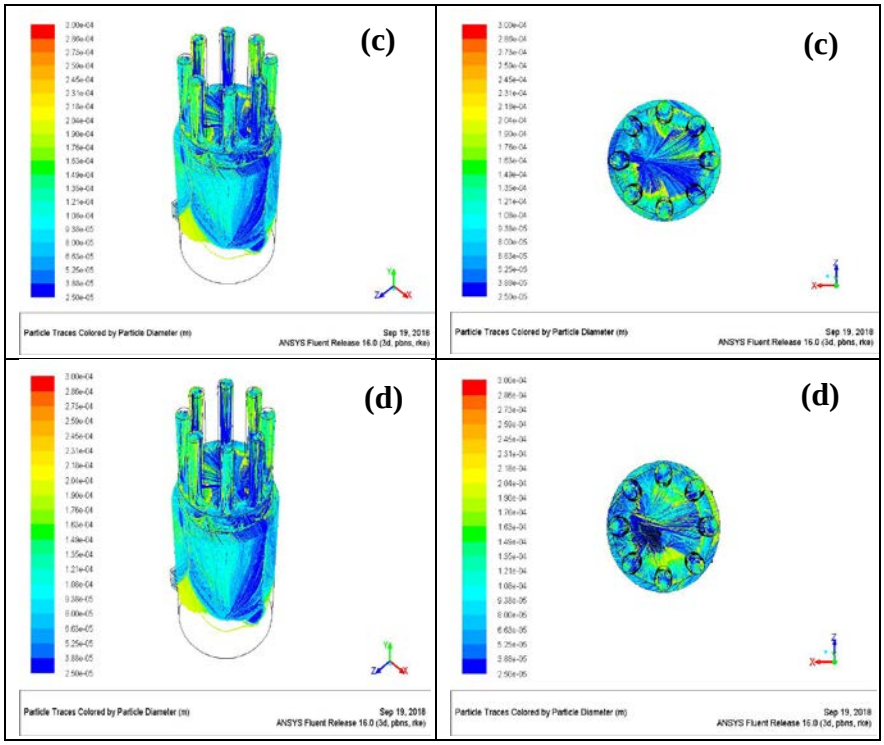

Fig. 11. Flow pattern of the injected coal particles and air inside the pulverizer at classifier blade angle of 70º (a), 60º (b), 50º (c) and 40º (d).

5. Conclusions

The two major highlights in this study are the effect of the classifier blade angle on both the quality and efficiency of classification. The maximum classification efficiency of 98.06% is observed for classifier blade angle of 70º meanwhile the lowest classification efficiency of 93% was achieved by the steepest classifier blade angle of 40º. Therefore, it can be concluded that the steepness of the classifier blade angle is inversely related to the classification efficiency.

Meanwhile, the quality of classification increases from 56.7% to 61.7% as the steepness of the classifier blade angle is reduced from 70 to 40 degrees. Thus, the steepness of the classifier blade angle is directly proportional to the quality of classification. The steeper angle of the blade diminishes the surface area available for particles to escape and increases the collision between coal particles and the classifier blades. Larger coal particles have higher gravitational force acting upon them and loss of momentum due to collisions among particles that could send the coal particles back for regrinding.

The overall findings from this study highlight promising findings for optimization of actual coal pulverisers. The conclusive highlights could be also beneficial for optimizing power plants to reduce concentration of harmful waste in unburnt ash, reduce regrinding costs, and optimize operational conditions in the boiler.

Acknowledgement

The authors would like to express gratitude to power generation unit, institute of power engineering, Universiti Tenaga Nasional (UNITEN) and Tenaga Nasional Berhad (TNB) for providing research grant to carry out this research.

Nomenclatures

Class Eff.	Classification efficiency
X	Particle diameter,μm

Greek Symbols

θ	Classifier blade angle

Abbreviations

CFD	Computational fluid dynamics
CKP mill	Roller-race mill without air classifier
DPM	Discrete phase model
E-mill	Ball-race mill
IEO2013	International Energy Outlook 2013
MPS	Roller-race mill
MW(e)	Megawatt end-user
RKE	Realizable k-epsilon Turbulence Model
RNG	Re-Normalisation Group k-epsilon Turbulence Model
RSM	Reynolds stress model

References

1. Zhang, X. (2016). *Emission standards and control of PM2.5 from coal-fired power plant*. London: Report No. CCC/267, IEA Clean Coal Centre.
2. Afolabi, J.L. (2012). *The performance of a static coal classifier and its controlling parameters*. Ph.D. Thesis, Dept. of Engineering, University of Leicester, Leicester, United Kingdom.
3. Chandrasekharan, S.; Panda Rames, C.; and Swaminathan Bhuvaneswari, N. (2014). Modeling, identification, and control of coal-fired thermal power plants. *Reviews in Chemical Engineering*, 30(2), 217.
4. Hansen-Carlson, J.; and Das, A. (in press). Settling characteristics and separation features in a CrossFlow separator for fine coal beneficiation. *International Journal of Coal Preparation and Utilization*.
5. Vuthaluru, H.B.; Pareek, V.K.; and Vuthaluru, R. (2005). Multiphase flow simulation of a simplified coal pulveriser. *Fuel Processing Technology*, 86(11), 1195-1205.
6. Bilirgen, H. (2005). *Balancing of Pulverized Coal Flows to Burners in Boilers with Pressurized Vertical Spindle Mills*. Bethlehem: DOE Award Number DE-FC26-03NT41867, Energy Research Center, Lehigh University.
7. Chandraker, A.L.; Panwalkar, A.S.; and Bhasker, C. (1995). Air flow studies in bowl mill housing. *22nd Fluid Mechanics and Fluid Power Conference.* IIT/Madras, India, 419–224.
8. Shi, F.; Kojovic, T.; and Brennan, M. (2015). Modelling of vertical spindle mills. Part 1: Sub-models for comminution and classification. *Fuel*, 143, 595-601.

9. Storm, S.K.; Storm, R.F.; Storm, D.S.; Tuzenew, S.; and McClellan, A. (2006). A Case Study of How Vertical Spindle Pulverizer Performance is Related to Overall Plant Performance. *ASME 2006 Power Conference*. Georgia, USA, 207-213.
10. Al-Muhsen, N.F.O.; Huang, Y.; and Hong, G. (2019). Effects of direct injection timing associated with spark timing on a small spark ignition engine equipped with ethanol dual-injection. *Fuel*, 239, 852-861.
11. Masum, B.M.; Masjuki, H.H.; Kalam, M.A.; Rizwanul Fattah, I.M.; Palash, S.M.; and Abedin, M.J. (2013). Effect of ethanol–gasoline blend on NOx emission in SI engine. *Renewable and Sustainable Energy Reviews*, 24, 209-222.
12. Yang, Y.; Ge, L.; He, Y.; Xie, W.; and Ge, Z. (2019). Mechanism and Fine Coal Beneficiation of a Pulsating Airflow Classifier. *International Journal of Coal Preparation and Utilization*, 391, 20-32.
13. EIA (2013). *International Energy Outlook 2013 With Projection to 2040*. Washington: Report No. DOE/EIA-0484(2013), U.S. Energy Information Administration.
14. Özer, C.; Shi, F.; and Whiten, B. (2009). *Improving the efficiency of fine coal grinding circuits – Tarong power station sitework*. Brisbane: Project No. C15079, Australian Research Administration Pty Ltd.
15. Özer, C.E.; and Whiten, W.J. (2012). A multi-component appearance function for the breakage of coal. *International Journal of Mineral Processing*, 104-105, 37-44.
16. Özer, C.E.; Whiten, W.J.; and Lynch, A.J. (2016). A multi-component model for the vertical spindle mill. *International Journal of Mineral Processing*, 148, 155-165.
17. Parham, J.J.; and Easson, W.J. (2003). Flow visualisation and velocity measurements in a vertical spindle coal mill static classifier. *Fuel*, 82(15-17), 2115-2123.
18. Johansson, R.; and Evertsson, M. (2012). CFD simulation of a gravitational air classifier. *Minerals Engineering*, 33, 20-26.
19. Ataş, S.; Tekir, U.; Paksoy, M.A.; Çelik, A.; Çam, M.; and Sevgel, T. (2014). Numerical and experimental analysis of pulverized coal mill classifier performance in the Soma B Power Plant. *Fuel Processing Technology*, 126, 441-452.
20. Shah, K.V.; Vuthaluru, R.; and Vuthaluru, H.B. (2009). CFD based investigations into optimization of coal pulveriser performance: Effect of classifier vane settings. *Fuel Processing Technology*, 90(9), 1135-1141.
21. Wang, Q.; Melaaen, M.C.; and De Silva, S.R. (2001). Investigation and simulation of a cross-flow air classifier. *Powder Technology*, 120(3), 273-280.
22. Afolabi, L.; Aroussi, A.; and Isa, N.M. (2011). Numerical modelling of the carrier gas phase in a laboratory-scale coal classifier model. *Fuel Processing Technology*, 92(3), 556-562.
23. Liu, W. (2015). Sun Tracker: Design, Build and Test. *2015 IEEE 81st Vehicular Technology Conference (VTC Spring)*. Glasgow, United Kingdom, 1-5.

24. Fakourian, S.; Fry, A.; and Jasperson, T. (2018). Analysis of particle behavior inside the classifier of a Raymond Bowl Mill while co-milling woody biomass with coal. *Fuel Processing Technology*, 182, 95-103.
25. Li, J.; Paul, M.C.; and Czajka, K.M. (2016). Studies of Ignition Behavior of Biomass Particles in a Down-Fire Reactor for Improving Co-firing Performance. *Energy & Fuels*, 307, 5870-5877.
26. Moazzem, S.; Rasul, M.; and Khan, M.M. (2012). *A Review on Technologies for Reducing CO2 Emission from Coal Fired Power Plants*. Queensland: InTech.
27. Varley, J. (2019). Manjung Power Plant, Perak. Retrieved December 10, 2019, from https://www.nsenergybusiness.com/projects/manjung-power-plant-perak/.
28. ANSYS Fluent V16 User's Guide. ANSYS, 2017.
29. Noor, M.; Wandel, A.P.; and Yusaf, T. (2013). Detail guide for CFD on the simulation of biogas combustion in bluff-body mild burner. *Proceedings of the 2nd International Conference of Mechanical Engineering Research (ICMER 2013)*, Pahang, Malaysia, 1-25.
30. Wang, Y.; Williams, K.; Jones, M.; and Chen, B. (2017). CFD simulation methodology for gas-solid flow in bypass pneumatic conveying – A review. *Applied Thermal Engineering*, 125, 185-208.
31. Altun, O.; Toprak, A.; Benzer, H.; and Darilmaz, O. (2016). Multi component modelling of an air classifier. *Minerals Engineering*, 93, 50-56.